ISIT'2013 1569717603

Coded Cooperation Using Rate-Compatible Spatially-Coupled Codes

Lai Wei, Daniel J. Costello, Jr., and Thomas E. Fuja
Department of Electrical Engineering
University of Notre Dame
Notre Dame, IN 46556
Email: {lwei1, dcostel1, tfuja}@nd.edu

***Abstract*—This paper investigates the use of rate-compatible spatially-coupled codes for coded cooperation. Transmitting to the same destination, two source nodes cooperate to combat block fading; using rate-compatible spatially-coupled codes, one source node relays additional parity-check bits for its partner's latest transmission to provide cooperative diversity at the destination. Different families of spatially-coupled codes are generated by applying the edge spreading technique to several rate-compatible protograph-based block LDPC codes from the literature. Simulation of the outage behavior shows that, using spatially-coupled codes, system performance approaches the theoretical limit, regardless of whether the original underlying block LDPC codes were designed specifically for coded cooperation or not. The same result holds when windowed decoding, instead of decoding across the entire graph, is used to reduce decoding latency.**

I. Introduction

Cooperative communication [1] organizes single-antenna sources so they share their resources in a way that enables full spatial transmit diversity to ameliorate fading. A typical scenario is shown in Figure 1, with two source nodes and one destination node. The main difference between this and a three-node relay system [2] is that Nodes A and B act as both a *source* and a *relay*, i.e., they each transmit newly-generated "local" data and also re-transmit data containing the partner's local information, whenever possible.

To carry out this dual role, Laneman *et al.* [1] proposed amplify-and-forward and decode-and-forward (DF) protocols based on time sharing; local and relayed data are concatenated and thus partition the transmit time axis. A variant of DF, called "coded cooperation" [3], incorporates channel coding into relaying by having each source transmit *additional parity-check bits* for its partner instead of simply repeating its partner's data. In this way, the destination benefits from information accumulation rather than SNR accumulation and thus achieves a lower outage probability compared with a repetition-based system.

Rate compatible codes are obviously good candidates for use in coded cooperation, since it is straightforward to partition a low-rate codeword into two parts and adjust the resource allocation between source and relay. Rate-compatible convolutional codes were used in [3], while [4] focused on the design of rate-compatible low-density parity-check (LDPC) codes to achieve a diversity order of two. In this paper, spatially-coupled LDPC codes are used for coded cooperation to exploit their capacity-achieving performance on general binary memoryless symmetric (BMS) channels.

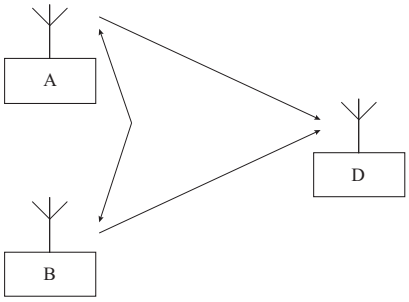

Fig. 1. Source nodes A and B cooperate to convey their data to a common destination Node D.

Terminated LDPC convolutional codes [5], or spatially-coupled codes [6], have belief-propagation (BP) decoding thresholds that saturate to the maximum *a-posteriori* (MAP) threshold of the underlying LDPC block code as the termination length grows. This phenomenon, called "threshold saturation", has been reported for a variety of code ensembles and channel models. In particular, Uchikawa *et al.* [2] designed several spatially-coupled protograph-based code ensembles for the binary erasure relay channel, and spatially-coupled versions of the MacKay-Neal (MN) codes are shown to achieve the capacity of this channel. In [7] Schwandter *et al.* designed bilayer spatially-coupled codes for a network with two sources, one relay and one destination, also for the binary erasure relay channel, and these codes achieve the Shannon limit under both symmetric and asymmetric channel conditions.

The main contribution of this paper is to extend the use of spatially-coupled codes to coded cooperation systems in which:

1) When serving as a relay, the transmitter switches intelligently between cooperative and non-cooperative transmission modes, and
2) Signals are corrupted by block fading with complex-valued additive white Gaussian noise (AWGN).

This work was supported in part by the U.S. National Science Foundation under grant CCF-1161754.

In what follows, Section II introduces the system model and Section III briefly describes the structure of rate-compatible protograph-based spatially-coupled code families. Section IV gives simulation results for the outage performance, and some conclusions are drawn in Section V.

II. System Model

As shown in Figure 1, two source ("*S*") nodes (A and B) cooperate to convey their data to a common destination D. Assume that time is slotted and each slot is further divided into two phases – a *local* phase followed by a *relay* phase. Within each phase, Node A first transmits, followed by Node B – so each time slot comprises four transmissions, two in the local phase and two in the relay phase.

Without loss of generality, consider Node A's transmission in a given time slot. During the first half of the local phase, Node A generates a new block of K information bits and encodes them into an N-bit codeword C_A, using a rate-compatible code. C_A is comprised of two parts: $C_A = [C_{A,1}, C_{A,2}]$ where $C_{A_1} \in \{0,1\}^{N_1}$, $C_{A_2} \in \{0,1\}^{N_2}$, and $N_1 + N_2 = N$. Thus, $C_{A,1}$ is a high-rate codeword embedded in the low-rate codeword C_A, and $C_{A,2}$ forms additional parity-check bits for $C_{A,1}$. Node A transmits the BPSK-modulated symbols of $C_{A,1}$, denoted as $x_{A,1} = \text{mod}_{\text{BPSK}}(C_{A,1})$, to complete its role in the local phase; Node B then operates analogously.

During the relay phase, if Node A has successfully decoded the K bits generated by Node B during the local phase – i.e., if $C_{B,1}$ can be recovered by Node A – then Node A generates $C_{B,2}$ and transmits $x_{A,2} = \text{mod}_{\text{BPSK}}(C_{B,2})$. Otherwise, Node A transmits its *own* additional parity check bits as $x_{A,2} = \text{mod}_{\text{BPSK}}(C_{A,2})$.

The overall spectral efficiency η (bits/symbol) is equal to K/N, the rate of the low-rate code. A key parameter for coded cooperation, called the "cooperation level", is defined as

$$\beta = \frac{N_2}{N}.$$

Corollary 1 in [4] states a necessary condition for a two-user coded cooperation system to achieve full diversity:

$$\eta \leq \min\{\beta, 1-\beta\}.$$

All four channels – A-to-B, B-to-A, A-to-D, and B-to-D – are corrupted by complex-valued AWGN and block Rayleigh fading, i.e., the fading remains constant over a time slot and varies independently from one time slot to another. We assume that perfect channel information (the realized fading factor and the average noise variance N_0) is available at the receiver.

There are four states in which Node D's receiver can operate. Take as an example Node D's decoding of Node A's codeword. Let $y_{S,i}$, $S \in \{A, B\}$ and $i \in \{1, 2\}$, denote the faded, noisy version of $x_{S,i}$.

1) State $\mathcal{S}_0$: Nodes A and B both transmitted in non-cooperative mode. There is no cooperative diversity and Node D decodes C_A based on $y_A = [y_{A,1}, y_{A,2}]$.
2) State $\mathcal{S}_1$: Node A transmitted in non-cooperative mode, but Node B was cooperative. There is cooperative diversity, and decoding of $C_{A,2}$ is enhanced by maximal ratio combining (MRC) of $y_{A,2}$ and $y_{B,2}$.
3) State $\mathcal{S}_2$: Node A transmitted in cooperative mode, but Node B was non-cooperative. Again, there is no cooperative diversity for Node A's data and Node D decodes the high-rate codeword $C_{A,1}$ based only on $y_{A,1}$.
4) State $\mathcal{S}_3$: Both Nodes A and B transmitted in cooperative mode, and Node D decodes C_A based on $[y_{A,1}, y_{B,2}]$. Again, there is cooperative diversity, since $C_{A,1}$ and $C_{A,2}$ experience independent block fading and complex-valued AWGN.

To operate in the correct state, Node D must know the transmission modes of Nodes A and B during the relay phase. (Alternatively, Node D could decode assuming each of the four states sequentially and use the code's error detection capability to determine which state yields correct results.) As in [8], this paper assumes Node D has access to the mode information it needs to determine the correct state.

III. Rate-Compatible Protograph-Based Spatially-Coupled Codes

This section briefly reviews the structure of two rate-compatible protograph-based spatially-coupled code families.

A. Protograph-Based Codes and Edge Spreading

A protograph-based code is derived from a small Tanner graph (the "protograph") by employing the "copy-and-permute" procedure: The protograph is first copied M times and then edges of the same type are permuted among the copies to generate a large "derived" graph. (M is called the "lifting" factor.) This is equivalent to replacing the nonzero elements in the base parity-check matrix $\mathbf{B}$ representing the protograph with an $M \times M$ permutation matrix (or a sum of non-overlapping $M \times M$ permutation matrices) and replacing the zero elements with the $M \times M$ all-zero matrix. Due to the construction procedure, the degree distribution of the protograph is maintained in the derived graph, so threshold analysis of the code ensemble using, for example, density evolution, can be carried out based on the protograph.

Lentmaier *et al.* [9] introduced a technique called "edge spreading" to describe the convolutional counterpart of a block code ensemble. A protograph with c variable nodes and $(c-b)$ check nodes with base matrix $\mathbf{B}$ is decomposed into $(1+m_s)$ base component matrices $\mathbf{B}_i$, where $i = 0, 1, 2, \ldots, m_s$ and

$$\mathbf{B} = \sum_{i=0}^{m_s} \mathbf{B}_i.$$

The infinite-length convolutional code ensemble can be represented by a doubly-infinite convolutional base matrix $\mathbf{B}_{[-\infty,\infty]}$ with a diagonal structure, as described in [9]. Essentially, variable node edges originally constrained to time t are now spread to connect to check nodes at times $t, t+1, \ldots, t+m_s$, and m_s is called the code memory.

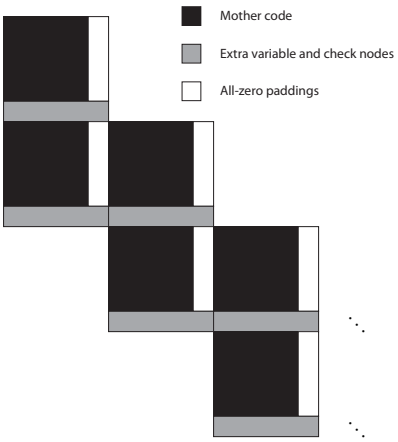

Fig. 2. Structure of an RC-SC code with $m_s = 1$. Note that the additional variable nodes are only connected to the additional check nodes.

In practice, encoding starts at some time, say $t = 1$, and terminates at some later time, say $t = L$, and we obtain a spatially-coupled code ensemble represented by the base matrix

$$\mathbf{B}_{[1,L]} = \begin{bmatrix} \mathbf{B}_0 & & & \\ \mathbf{B}_1 & \mathbf{B}_0 & & \\ & \mathbf{B}_1 & \ddots & \\ & & \ddots & \mathbf{B}_0 \\ & & & \mathbf{B}_1 \end{bmatrix},$$

where $m_s = 1$ in this example and the design rate is given by

$$R = 1 - \frac{(c-b)\cdot(L+m_s)}{c\cdot L},$$

which converges to b/c as $L \to \infty$, i.e., the rate loss due to termination vanishes as the termination length L increases.

B. Rate-Compatible Spatially-Coupled Codes

Rate-compatible (RC) *spatially-coupled* (SC) codes can be derived from RC block code families reported in the literature, e.g., the RC protograph-based Raptor-like (RC-PBRL) codes and the RC punctured-node PBRL (RC-PN-PBRL) codes from [10], and the RC root-LDPC (RCR-LDPC) codes from [4]. All three code families fit into the protograph structure, and their rate compatibility is achieved by "extending" – i.e., by adding extra parity bits to a high-rate mother code to produce lower-rate codes [11]. Figure 2 illustrates this technique for an RC-SC code with $m_s = 1$; note that *every* $\mathbf{B}_0$ and *every* $\mathbf{B}_1$ are extended.

We focus on the RC-SC-PBRL and the RC-SC-PN-PBRL code families in this paper. Similar results have been observed for SC codes with $m_s = 1$ and 2 generated using the $(3, 9, 3, 6)$-regular RCR-LDPC code from [4], which was specifically designed for coded cooperation.

C. The RC-SC-PBRL and the RC-SC-PN-PBRL Codes

An RC-PBRL code [10] can be represented by the base matrix

$$\mathbf{B}^{(k)} = \left[\begin{array}{c|c} \left(\mathbf{B}^{(1)}\right)_{(c_1-b)\times c_1} & \mathbf{0}_{(c_1-b)\times(k-1)} \\ \hline \left(\mathbf{B}^{(e,2)}\right)_{1\times c_1} & \\ \vdots & \mathbf{I}_{k-1} \\ \left(\mathbf{B}^{(e,k)}\right)_{1\times c_1} & \end{array}\right]_{(c_k-b)\times c_k},$$

where $c_k = c_1 + (k-1)$ for incremental redundancy step $k = 2, \ldots, 11$, and I_{k-1} is a size-$(k-1)$ identity matrix. An RC-SC-PBRL code with $m_s = 1$ was first presented in [12], where details of the base component matrices can be found. An RC-SC-PN-PBRL code with $m_s = 1$ based on the RC-PN-PBRL code in [10] can be constructed in a similar way, such that

1) $\{\mathbf{B}_i^{(e,k)}\}_{k=2}^{11}$ for $i = 0, 1$ are the same as those of the RC-SC-PBRL code.
2) All-zero checks at time L result in a small increase in the design rate, which, similar to the rate loss, vanishes as $L \to \infty$.
3) The first variable node at each time instant is always punctured, so that the rates are the same as for the RC-SC-PBRL code.

IV. Outage Performance

In this section, the outage behavior of the coded cooperation system is evaluated in two ways:

1) Using BPSK capacity: An outage occurs when the instantaneous channel capacity falls below the spectral efficiency η. We refer to this as "capacity outage."
2) Using the RC-SC code threshold: An outage occurs when the instantaneous channel condition (characterized by E_s/N_0) falls below the belief propagation decoding threshold θ; we refer to this as "code outage." Here, θ is calculated via density evolution using the reciprocal channel approximation (RCA) method which, for protograph-based codes, is described in [13].

The system outage ("O") probability at Node D is given by

$$P_O = \sum_{i=0}^{3} P_O(\text{state } i)\cdot P(\text{state } i).$$

The state distribution $P(\text{state } i)$ is determined by the transmission modes, which in turn depend on the outage behavior at the source nodes.

For the RC-SC-PBRL and the RC-SC-PN-PBRL code families analyzed below, we let the termination length $L = 100$.

The $k = 11$ code with spectral efficiency $\eta = 0.3278$ is selected as the low-rate code. The $k = 2$, 3, 4, 5, and 6 codes are used for high-rate transmission during the local phase, resulting in cooperation levels $\beta = 5/9$, $1/2$, $4/9$, $7/18$, and $1/3$, respectively.

TABLE I
THRESHOLDS USING THE RC-SC-PBRL CODE
(AWGN SYMBOL ENERGY-TO-NOISE RATIO E_s/N_0)

β	5/9	1/2	4/9	7/18	1/3
θ_{source}	1.1483	0.8745	0.7162	0.6109	0.5327
$\theta_{\mathcal{S}_0}$	0.3139	0.3139	0.3139	0.3139	0.3139
$\theta_{\mathcal{S}_2}$	1.1483	0.8745	0.7162	0.6109	0.5327

Table I shows the AWGN channel thresholds of the RC-SC-PBRL code (1) at a source node ("θ_{source}"), (2) in state $\mathcal{S}_0$ at Node D ("$\theta_{\mathcal{S}_0}$"), and (3) in state $\mathcal{S}_2$ at Node D ("$\theta_{\mathcal{S}_2}$"), for different values of β. As expected:

1) $\theta_{\mathcal{S}_0}$ is constant, because the same low-rate code is used.
2) $\theta_{\text{source}} = \theta_{\mathcal{S}_2}$, because in both cases one high-rate codeword is decoded.
3) θ_{source} improves as β decreases, because more resources are dedicated to transmitting local bits during the local phase when β is small.

Figure 3 shows $\theta_{\mathcal{S}_1}$ and $\theta_{\mathcal{S}_3}$ for the case $\beta = 1/2$. Cooperative diversity is achieved in $\mathcal{S}_1$ and $\mathcal{S}_3$, so the threshold is determined by the source ("S")-to-destination channel and the relay ("R")-to-destination channel simultaneously, i.e., $\theta_{\mathcal{S}_1} = (\theta_{\mathcal{S}_1}(\text{S}), \theta_{\mathcal{S}_1}(\text{R}))$. For comparison, the BPSK capacity is also shown. It is observed that in both states, the gap between threshold and capacity is approximately uniform. Also note that when $\theta_{\mathcal{S}_1}(\text{R}) = 0$, $\theta_{\mathcal{S}_1}(\text{S}) = \theta_{\mathcal{S}_0}$, and when $\theta_{\mathcal{S}_3}(\text{R}) = 0$, $\theta_{\mathcal{S}_3}(\text{S}) = \theta_{\mathcal{S}_2}$.

Figure 4 shows $\theta_{\mathcal{S}_1}$ and $\theta_{\mathcal{S}_3}$, respectively, for different β. For $\theta_{\mathcal{S}_1}$,

1) When $\theta_{\mathcal{S}_1}(\text{S}) = 0$, $\theta_{\mathcal{S}_1}(\text{R})$ improves as β increases, because the information is transmitted from relay to destination only, and a larger β means that more resources are dedicated to this channel.
2) When $\theta_{\mathcal{S}_1}(\text{R}) = 0$, $\theta_{\mathcal{S}_1}(\text{S})$ is the same for different β. This is because the relay-to-destination channel does not contribute to decoding and hence has no influence on the decoding threshold at Node D.

Similarly, for $\theta_{\mathcal{S}_3}$,

1) When $\theta_{\mathcal{S}_3}(\text{S}) = 0$, $\theta_{\mathcal{S}_3}(\text{R})$ improves as β increases.
2) When $\theta_{\mathcal{S}_3}(\text{R}) = 0$, $\theta_{\mathcal{S}_3}(\text{S})$ improves as β decreases, because the information is transmitted from source to destination only, and a smaller β means that more resources are dedicated to this channel.
3) The thresholds for different β cross at the point $\theta_{\mathcal{S}_3}(\text{S}) = \theta_{\mathcal{S}_3}(\text{R})$, since this is equivalent to transmitting the whole low-rate codeword through a *single* channel.

Figure 5 shows the system outage probability for the RC-PBRL, RC-PN-PBRL, RC-SC-PBRL, and RC-SC-PN-PBRL code families, along with the corresponding BPSK capacity outage probability, where the SC codes suffer a small rate loss due to termination.[1] It is observed that

[1]In contrast to Figures 3 and 4, it is convenient to use a logarithmic scale in Figure 5 and to express the average bit energy-to-noise-ratio E_b/N_0 in dBs.

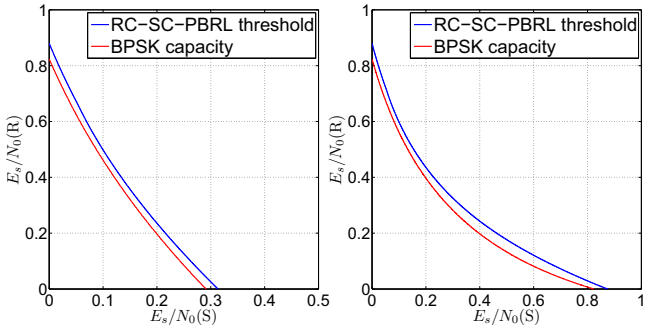

(a) $\mathcal{S}_1$ (b) $\mathcal{S}_3$

Fig. 3. Thresholds of the RC-SC-PBRL code compared with the BPSK capacity in (a) state $\mathcal{S}_1$ and (b) state $\mathcal{S}_3$ at Node D. $\beta = 1/2$, $\eta = 0.3278$.

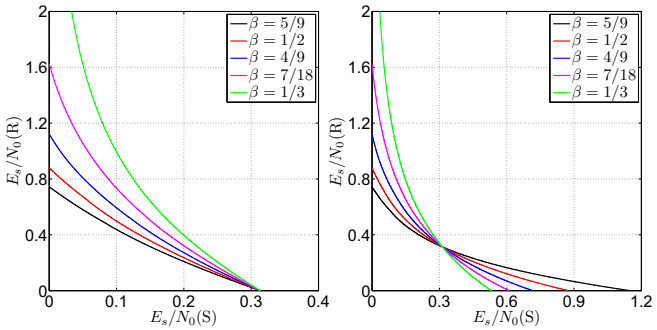

(a) $\mathcal{S}_1$ (b) $\mathcal{S}_3$

Fig. 4. Thresholds of the RC-SC-PBRL code in (a) state $\mathcal{S}_1$ and (b) state $\mathcal{S}_3$ at Node D. $\eta = 0.3278$.

1) The SC codes perform better than the underlying block codes and exhibit capacity-approaching behavior because of the threshold saturation phenomenon [6]. At outage probability 10^{-2}, RC-SC-PBRL provides 0.60 dB gain over RC-PBRL, while RC-SC-PN-PBRL provides 0.54 dB gain over RC-PN-PBRL. Also, the gaps between the SC code outage probabilities and the BPSK capacity outage probability (for $\eta = 0.3278$) are approximately uniform.
2) As in [10], RC-PN-PBRL codes perform better than RC-PBRL codes, and this property is inherited by their SC counterparts. However, the gap between RC-SC-PBRL and RC-SC-PN-PBRL (0.10 dB) is smaller than between RC-PBRL and RC-PN-PBRL (0.15 dB).
3) As $L \to \infty$, $\eta \to 1/3$. Based on simulations, we observe that the SC code outage probabilities for $L = 100$, 200, and 500 are almost indistinguishable, i.e., $L = 100$ is a very good estimate of the ultimate performance for $L \to \infty$. As a result, compared with the BPSK capacity outage probability for $\eta = 1/3$, we conclude that the SC codes offer near-capacity performance with no loss in spectral efficiency, even though the underlying block codes were not designed specifically for coded cooperation.

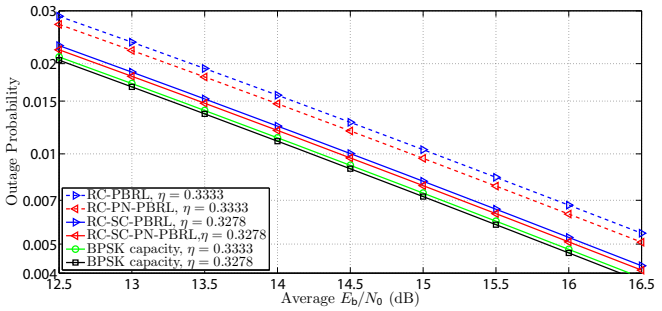

Fig. 5. Comparison of the system outage probability at Node D: RC-PBRL, RC-PN-PBRL, RC-SC-PBRL, and RC-SC-PN-PBRL. $\beta = 1/2$.

TABLE II
AVERAGE BIT ENERGY-TO-NOISE RATIO E_b/N_0 (IN DB) AT OUTAGE PROBABILITY 10^{-2}: RC-SC-PBRL, $\eta = 0.3278$

β	5/9	1/2	4/9	7/18	1/3
RC-SC-PBRL	15.60	14.67	13.94	13.69	13.67
BPSK Capacity	15.26	14.32	13.77	13.50	13.45
Gap	0.34	0.35	0.17	0.19	0.22

Table II shows the E_b/N_0 performance of the RC-SC-PBRL coded cooperation system at outage probability 10^{-2} when β varies, compared to the BPSK capacity. It is observed that, over the entire range of β, using the RC-SC-PBRL code provides performance within 2.5% of the theoretical limit.

Due to their convolutional structure, SC codes can be decoded using a windowed decoding (WD) scheme [14] [15], i.e., only those variable and check nodes within a window of size[2] W are updated during each BP iteration, and the window shifts across the graph until decisions have been made for all the variable nodes. Compared with treating the SC code as a block code and decoding across the entire graph, WD reduces latency at the expense of a (slight) loss in performance, depending on W. Table III shows the performance of the RC-SC-PBRL coded cooperation system with $\beta = 1/2$ at outage probability 10^{-2} when WD is used. It is observed that RC-SC-PBRL with $W = 5$ already outperforms RC-PBRL with the flooding schedule. Also, for RC-SC-PBRL, the outage probability improves as W increases, and $W = 10$ provides performance nearly the same as decoding across the entire graph, which, if treated as a special case of WD, has $W = L + m_s = 101$.

V. CONCLUSIONS

This paper investigated the use of spatially-coupled codes in a coded cooperation system; two families of protograph-based RC-SC codes were employed as examples. In each case, the results demonstrate that SC codes have significantly better outage performance than the underlying block codes and exhibit a small gap to capacity – both with a finite termination length L and as $L \to \infty$ – even though the underlying codes were not designed for coded cooperation. This is true even when a less-powerful windowed decoding scheme is used to reduce latency.

[2]The window size is defined in [14] [15].

TABLE III
AVERAGE E_b/N_0 (IN DB) AT OUTAGE PROBABILITY 10^{-2}: RC-SC-PBRL, $\beta = 1/2$, $\eta = 0.3278$, WD

	E_b/N_0	Gap
BPSK capacity, $\eta = 0.3278$	14.32	-
RC-SC-PBRL, $W = 5$	15.15	0.83
RC-SC-PBRL, $W = 10$	14.68	0.36
RC-SC-PBRL, $W = L + m_s = 101$	14.67	0.35
RC-PBRL, $\eta = 0.3333$	15.27	-

REFERENCES

[1] J. N. Laneman, D. N. C. Tse, and G. W. Wornell, "Cooperative Diversity in Wireless Networks: Efficient Protocols and Outage Behavior," *IEEE Transactions on Information Theory,* Vol. 50, No. 12, pp. 3062-3080, December 2004.

[2] H. Uchikawa, K. Kasai, and K. Sakaniwa, "Spatially Coupled LDPC Codes for Decode-and-Forward in Erasure Relay Channel," *2011 IEEE International Symposium on Information Theory (ISIT) Proceedings*, pp. 1474-1478, Saint Petersburg, Russia, July 31-August 5, 2011.

[3] T. E. Hunter and A. Nosratinia, "Diversity Through Coded Cooperation," *IEEE Transactions on Wireless Communications,* Vol. 5, pp. 283-289, Feburary 2006.

[4] D. Duyck, J. J. Boutros, and M. Moeneclaey, "Low-Density Graph Codes for Coded Cooperation on Slow Fading Relay Channels," *IEEE Trans. on Information Theory,* Vol. 57, No. 7, pp. 4202-4218, July 2011.

[5] M. Lentmaier, A. Sridharan, D. J. Costello, and K. Sh. Zigangirov, "Iterative Decoding Threshold Analysis for LDPC Convolutional Codes," *IEEE Transactions on Information Theory*, Vol 56, No. 10, pp. 5274-5289, October 2010.

[6] S. Kudekar, T. J. Richardson, and R. L. Urbanke, "Threshold Saturation via Spatial Coupling: Why Convolutional LDPC Ensembles Perform So Well over the BEC," *IEEE Transactions on Information Theory,* Vol. 57, No. 2, pp. 803-834, February 2011.

[7] S. Schwandter, A. Graell i Amat, G. Matz, "Spatially Coupled LDPC Codes for Two-User Decode-and-Forward Relaying," *2012 7th International Symposium on Turbo Codes & Iterative Information Processing* (ISTC), Gothenburg, Sweden, August 2012.

[8] S. V. Maiya and T. E. Fuja, "Cooperation via Trellis Pruning," *IEEE Trans. on Communications,* Vol. 59, No. 6, pp. 1563-1569, June 2011.

[9] M. Lentmaier, G. P. Fettweis, K. S. Zigangirov, and D. J. Costello, "Approaching Capacity with Asymptotically Regular LDPC Codes," *Information Theory and Applications Workshop* (ITA), San Diego, California, February 2009.

[10] T. Y. Chen, D. Divsalar, J. Wang, and R. Wesel, "Protograph-Based Raptor-Like LDPC Codes for Rate Compatibility with Short Block-lengths," *2011 IEEE Global Communications Conference* (GLOBECOM), Houston, TX, U.S., Dec. 2011.

[11] M. R. Yazdani and A. H Banihashemi, "On Construction of Rate-Compatible Low-Density Parity-Check Codes," *IEEE Communications Letters,* Vol. 8, No. 3, pp. 159-161, March 2004.

[12] W. Nitzold, M. Lentmaier, and G. P. Fettweis, "Spatially Coupled Protograph-Based LDPC Codes for Incremental Redundancy," *2012 7th International Symposium on Turbo Codes & Iterative Information Processing* (ISTC), Gothenburg, Sweden, August 2012.

[13] D. Divsalar, S. Dolinar, C. R. Jones, and K. Andrews, "Capacity-Approaching Protograph Codes," *IEEE Journal on Selected Areas in Communications,* Vol. 27, No. 6, pp. 876-888, August 2009.

[14] A. R. Iyengar, M. Papaleo, P. H. Siegel, J. K. Wolf, A. Vanelli-Coralli, and G. E. Corazza, "Windowed Decoding of Protograph-Based LDPC Convolutional Codes Over Erasure Channels," *IEEE Transactions on Information Theory,* Vol. 58, No. 4, pp. 2303-2320, April 2012.

[15] M. Lentmaier, M. M. Prenda, and G. P. Fettweis, "Efficient Message Passing Scheduling for Terminated LDPC Convolutional Codes," *2011 IEEE International Symposium on Information Theory (ISIT) Proceedings*, pp. 1826-1830, Saint Petersburg, Russia, July 31-August 5, 2011.